ECCOMAS Congress 2016
VII European Congress on Computational Methods in Applied Sciences and Engineering
M. Papadrakakis, V. Papadopoulos, G. Stefanou, V. Plevris (eds.)
Crete Island, Greece, 5–10 June 2016

SHAPE IDENTIFICATION ANALYSIS OF CAVITY IN RESIN STRUCTURE BASED ON THERMAL NONDESTRUCTIVE TESTING METHOD

K. Maruoka[1], **T. Kurahashi**[2], **and T. Iyama**[3]

[1] Graduate School of Nagaoka University of Technology
1603-1 Kamitomioka, Nagaoka, Niigata, Japan
e-mail: s133075@stn.nagaokaut.ac.jp

[2] Nagaoka University of technology
1603-1 Kamitomioka, Nagaoka, Niigata, Japan
e-mail: Kurahashi@mech.nagaokaut.ac.jp

[3] Nagaoka National College of Technology
888 Nishikatakai, Nagaoka, Niigata, Japan
e-mail: iyama@nagaok-ct.ac.jp

Keywords: Shape identification analysis, Thermal nondestructive testing method, Finite element method, Adjoint variable method, Gaussian filter.

Abstract. *The shape identification analysis is carried out to obtain the unknown defects shape in the structure based on the finite element and the adjoint variable methods. In this study, the test piece including the known defect shape is employed to solve the shape identification problem. In addition, we present the shape identification problem of cavity in resin test piece made by 3D printer using the observed temperature on the test piece surface. It is known that the temperature on top of the test piece is not uniformly distributed, if there are cavities in the test piece. Furthermore, according to practical experiment, it has been confirmed that the characteristic of the temperature distribution depends on cavities size. The thermal physical constants, i.e., the thermal conductivity and the convection coefficient, are identified for the model of the test piece including a cavity based on the experimental data, and the shape identification analysis is carried out. In the numerical analysis, the finite element method is applied to simulate the temperature distribution in the test piece, and the adjoint variable method is employed to identify the cavity shape.*

1 INTRODUCTION

Thermal testing method is known as a kind of non-destructive testing for estimating corrosion in structures in fields of civil and mechanical engineering. This testing method is intended to find out existence of defects by thermal image of thermography. In addition, it has the advantage that can give defect inspection through the positon of surfaces. An example of a thermal image of the top surface of test piece having a cavity which is heated from the lower surface is shown in Figure 1. Then outer and inner test piece have different temperatures, being able to estimate that the test piece has a defect. However there are some cases too difficult to find out defects, depending on the size and depth of the defects. On the other hand, by applying a thermal testing method, studies to identify the defect shape by inverse analysis method from time history of temperature [1, 2] is carried out. In previous studies, it is concluded that the corrosion shape of the concrete can be identified if assuming the initial corrosion shape as appropriate. In the fields of optimal control problems, the study about reduction of convergence for performance function [3, 4].

In this study, we use the resin structure created by 3D printer such that the shape of cavity is freely changed. The purpose of this study is to identify the cavity shape based on the inverse analysis, and to carry out the improvement of the treatment in computation of the shape identification.

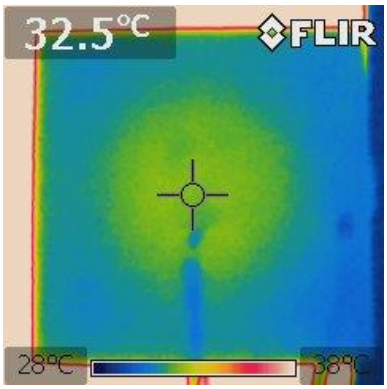

Figure 1: Heat image

2 EXPERIMENT BY THERMAL NONDESTRUCTIVE TESTING METHOD

2.1 Measurement situation

The photo of experiment is shown in Figure 2, and the drawing of test piece used this study is shown in Figure 3 (a). The sample has been made of ABS resin and created by 3D printer. Then a test piece with a cavity having a thickness of 10mm and a test piece without cavity are also created. Pair of test pieces (15mm thickness cavity, no cavity) are set on hot plate, heated up for 1200 seconds, and thermal observation at two observation points on the surface with a thermocouple is carried out every 10 seconds. Observation point is placed on the upper surface of the thick point (Point A) and thin portion (Point B) of the cavity thickness (See Figure 3(b)).

2.2 Observational result

The measured temperature history at Point A and Point B is shown in Figure 4 (a) and (b). As a result, without relation to presence or absence of the cavity, there are no big difference in temperature history observed at Point B. However, in Point A, it is confirmed a tendency that

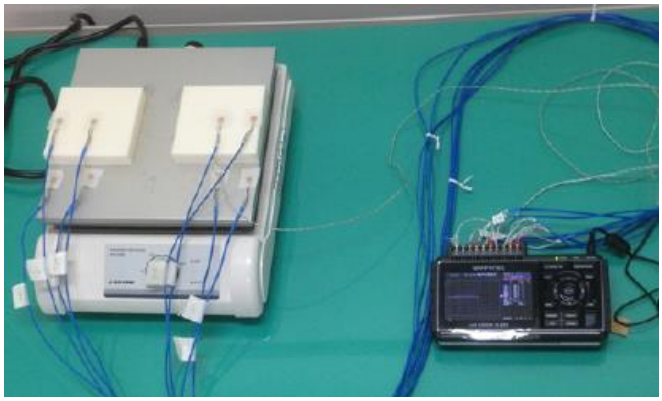

Figure 2: Photo of observation

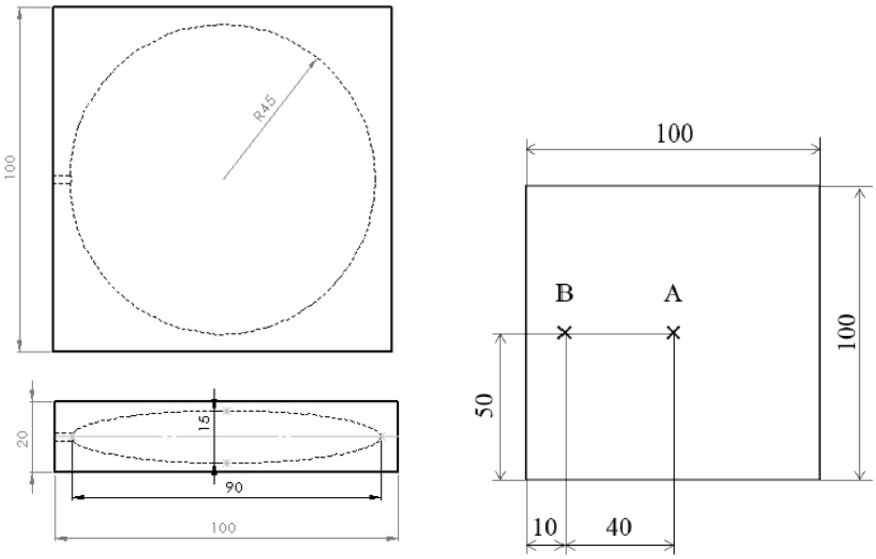

(a) Drawing of the test piece (b) Observation point

Figure 3: Detail of the test piece

the temperature of the test piece with a cavity increases more than the test piece without a cavity at the same time. This is considered to effect due to the influence of heat transfer from the air which is heated in the cavity. Similar experiment are also carried out using a test piece with a cavity having a thickness of 10mm. The temperature history measured at Point A and Point B is shown in Figure 5 (a) and (b). From the results, it is found that the temperature difference at Point A is small compared the case with a test piece cavity thickness 15mm. Thus, the thickness of the cavity difference, it can be seen that the result is a difference in the temperature history at the test piece surface.

3 SHAPE IDENTIFICATION ANALYSIS

Using thermal properties found out previous chapter, the shape identification analysis is carried out. Initial shape model is given as including the cavity thickness 13mm, we set target shape as cavity thickness 15mm.

3.1 State equation

Formulation in the shape identification analysis is described below. In this study, the whole domain of the test piece is denoted as Ω. Then temperature distribution ϕ satisfies heat transfer

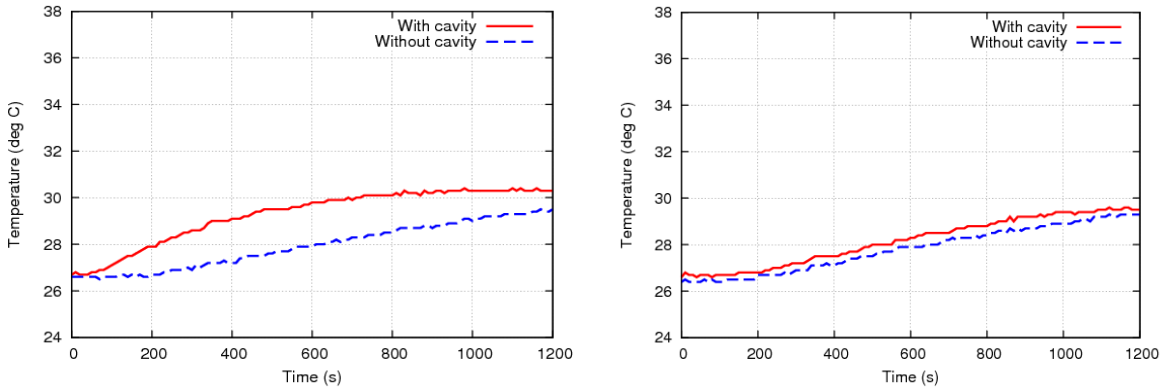

(a)At Point A (b) At Point B

Figure 4: Time history of temperature of resin surface (1)

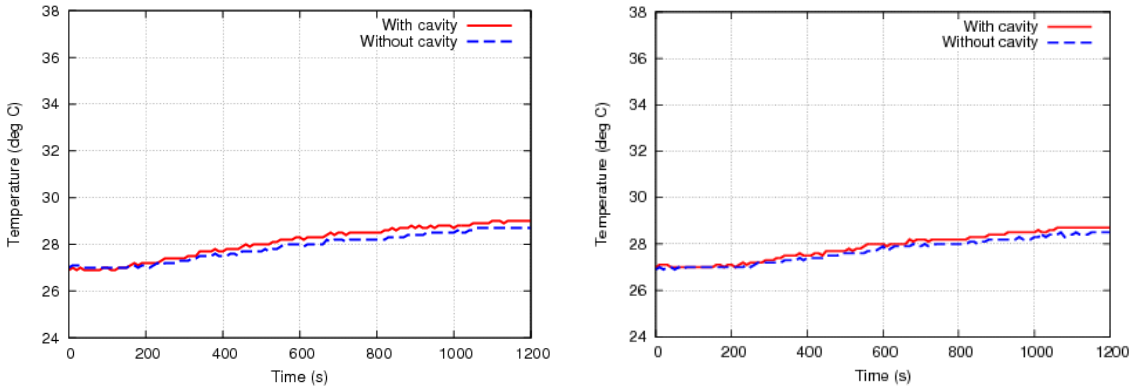

(a)At Point A (b) At Point B

Figure 5: Time history of temperature of resin surface (2)

equation shown in Equation (1). For the heat transfer equation, initial condition and boundary condition are defined as Equations (2).

$$\rho c\dot{\phi} - \kappa\phi_{,ii} = 0 \tag{1}$$

$$\begin{cases} \phi = \hat{\phi}(t_0) \quad in \quad \Omega \\ \phi = \hat{\phi} \quad on \quad \Gamma_1 \\ -\kappa\phi_{,i}n_i = h_1(\phi - \phi_{\inf}) \quad on \quad \Gamma_2 \\ -\kappa\phi_{,i}n_i = h_2(\phi - \phi_{cav}) \quad on \quad \Gamma_3 \end{cases} \tag{2}$$

where ρ, c, κ, n_i, h_1, h_2, $\phi_{\inf}$ and ϕ_{cav} denote density, specific heat, thermal conductivity, unit normal vector, heat transfer coefficient of inside cavity, heat transfer coefficient of outside surface, surrounding temperature, temperature inside cavity. Γ_1 means lower surface, Γ_2 means outside surfaces, and Γ_3 means surface of cavity (See Figure 6).

3.2 Performance function

To evaluate computed temperature history, following performance function is defined.

$$J = \frac{1}{2}\int_{t_0}^{t_f}\int_{\Omega} R(\phi - \phi_{obs})^2 \, d\Omega dt \tag{3}$$

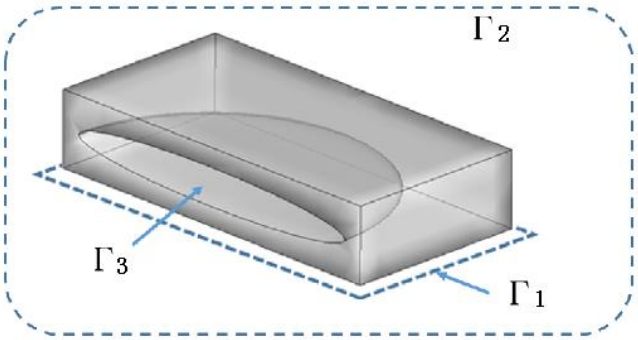

Figure 6: Boundary definition of the test piece

where t_f, R, and ϕ_{obs} mean heating termination time (Total time), weight diagonal matrix, observed temperature.

3.3 Lagrangian function

Applying adjoint variable λ, following Lagrangian function is obtained to minimize performance function [6, 7]. The adjoint variable method is one of the minimization technique of the performance function, and is suitable for the inverse problems such that a lot of unknown parameters should be solved.

$$J^* = J + \int_{t_0}^{t_f} \int_{\Omega} \lambda(\rho c\dot{\phi} - \kappa\phi_{,ii}) d\Omega dt \tag{4}$$

First variation which is necessary condition that Lagrangian function become minimization is shown in equation (5). Stationary condition is given as condition that each terms equal zero.

$$\delta J^* = \frac{\partial J^*}{\partial \lambda}\delta\lambda + \frac{\partial J^*}{\partial \dot{\phi}}\delta\dot{\phi} + \frac{\partial J^*}{\partial \phi}\delta\phi + \frac{\partial J^*}{\partial x_i}\delta x_i \tag{5}$$

where x_i indicates transplantable nodes.

3.4 Finite element equation

Shape function for four-node tetrahedral element is introduced into state equation to discretize the state equation spatially with Galerkin method. In addition, the equation is discretized in time based the Crank-Nicolson method. The finite element equation is shown in equation (6).

$$\rho c[\mathrm{M_e}]\{\dot{\phi}_e\} + \kappa[H_e]\{\phi_e\} = \{T_e\} \quad in \quad \Omega_e \tag{6}$$

In equation (6), [Me], [He], and {Te} indicate:

$$[M_e] = \int_{\Omega_e} \{\Phi_e\}\{\Phi_e\}^T d\Omega \tag{7}$$

$$[H_e] = \int_{\Omega_e} \{\Phi_{e,i}\}\{\Phi_{e,i}\}^T d\Omega \tag{8}$$

$$\{T_e\} = -\int_{\Gamma_2} q\{\Phi_e\} ds - \int_{\Gamma_3} q\{\Phi_e\} ds \tag{9}$$

where q means thermal flow late. Superposing finite element equation for individual domain, such equation can be represented as equation (10).

$$[A(x_i)]\{\dot{\phi}\}+[B(x_i)]\{\phi\}=\{C(x_i)\} \tag{10}$$

3.5 Adjoint equation

From the first variation of the Lagrangian function, following adjoint equation and conditions are obtained. This equation manifests oneself as adjoint problem to calculate λ.

$$-[\mathrm{A}]^{\mathrm{T}}\{\dot{\lambda}\}+[B]^{T}\{\lambda\}+[R]^{T}\{\phi-\phi_{obs}\}=\{S\} \quad in \quad \Omega_e \tag{11}$$

$$\begin{cases} \lambda(t_f)=0 & in \quad \Omega \\ \lambda=0 & on \quad \Gamma_1 \\ S=0 & on \quad \Gamma_2 \\ S=0 & on \quad \Gamma_3 \end{cases} \tag{12}$$

3.6 Gradient vector of the Lagrangian function

Final term in equation (5) can be calculated with adjoint variable as following equation:

$$\left\{\frac{\partial \mathrm{J}^{*}}{\partial x_i}\right\}=\int_{t_0}^{t_f}\{\lambda\}^{T}\left(\left[\frac{\partial \mathrm{A}}{\partial \mathrm{x_i}}\right]\{\dot{\phi}\}+\left[\frac{\partial \mathrm{B}}{\partial \mathrm{x_i}}\right]\{\phi\}-\left\{\frac{\partial C}{\partial \mathrm{x_i}}\right\}\right)dt \quad in \quad \Omega_e \tag{13}$$

Nodal positions are updated with gradient vector. In this method, the update of the coordinate on cavity surface and the re-evaluation of the temperature difference at observation points are iteratively carried out according to steepest descent method [7].

3.7 Computational condition

The finite element model of the test piece is shown in Figure 7. The model is composed four-node tetrahedral element. Total number of nodes are 1460, and total number of elements are 5552. The computational conditions are referred to experiment and given as Table 1. Thermal properties for the test piece is given as shown in Table 2 considering the thing which the ABS resin is not filled enough as shown in Figure 8. The observational data at Point A in the previous experiment (See Figure 4 (a)) is employed as observed temperature. In addition, the time history of temperature on the hot plate and temperature within the cavity as boundary conditions are shown in Figure 9 (a) and (b).

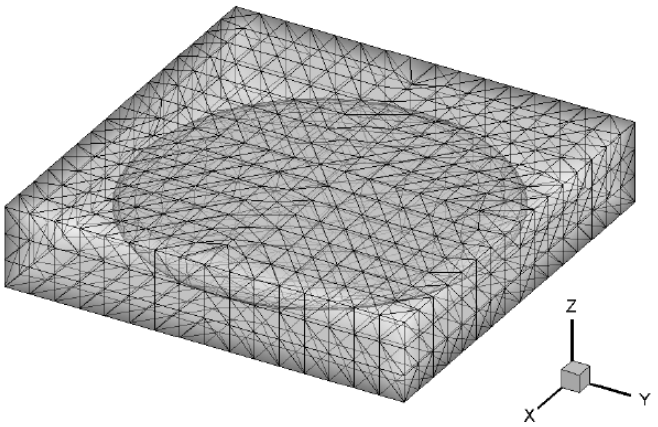

Figure 7: Finite element model

Total number of nodes	1460
Total number of elements	5552
Total time t_f, sec	600
Time increment Δt, sec	10
Time step	60
Convergence criterion ε	10^{-6}

Table 1: Computational condition.

	Density ρ	Specific heat c	Thermal conductivity κ	Heat transfer coefficient h	
	Kg/m^3	J/(kg℃)	W/(m^2℃)	Outside surface W/(m^2℃)	Cavity W/(m^2℃)
ABS	750	1386	0.1354	10.0	7.0

Table 2: Example of the construction of one table.

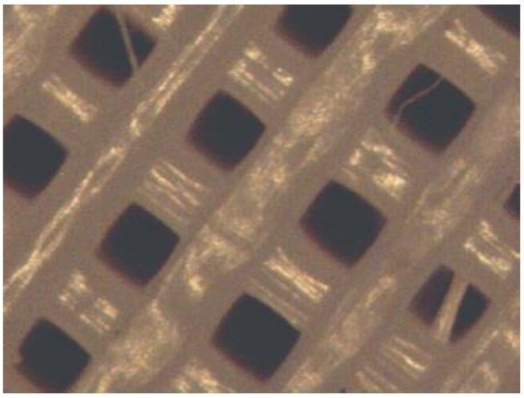

Figure 8: Cross-section of test piece

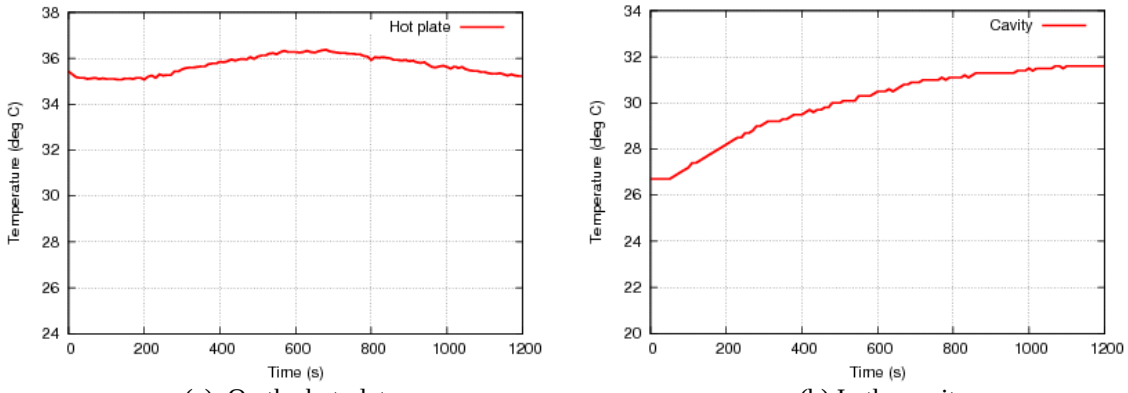

(a) On the hot plate (b) In the cavity

Figure 9: Time history of temperature of resin surface

3.8 Computational result

Figure 10 (a) shows identified shape of the cavity and Figure 10 (b) shows variation of normalized performance function per iteration number. Final iteration number is 18, performance function is about 0.55 when converting initial performance function into 1. However surface of the cavity becomes undulation, targeted shape as 15mm thickness cavity cannot be obtained.

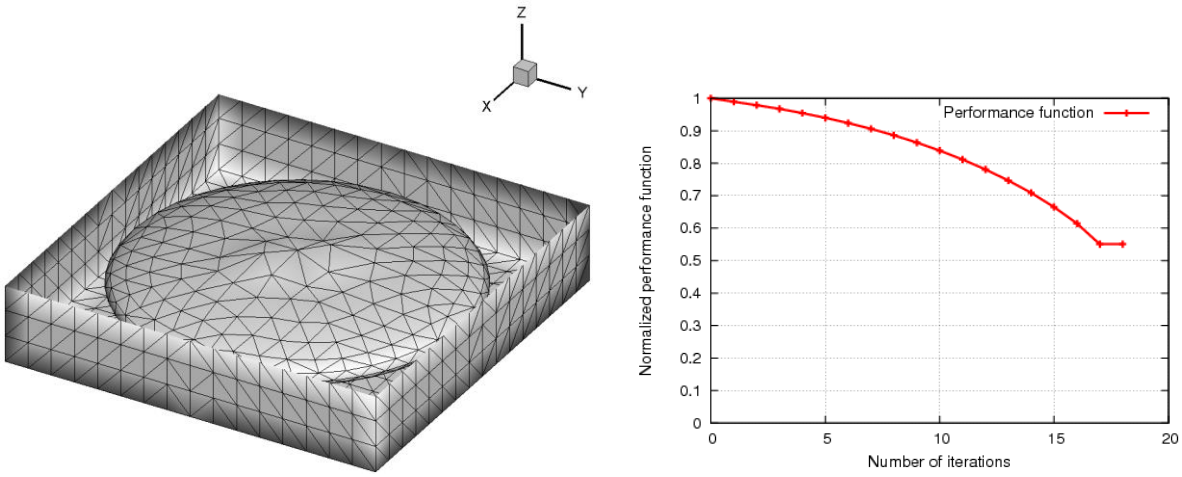

(a) The shape of the cavity at the final iteration (b) Variation of performance function

Figure 10: Computational results (1)

4 SMOOTHING PROCESS

The smoothing process for gradient vector is introduced to modify the oscillation of the gradient vector with respect to coordinate on cavity surface. For the smoothing method, Gaussian filter [8] is employed. Looking at the surface of the cavity as two-dimensional surface, the gradient vector is smoothed.

4.1 Gaussian filter

Gaussian filter is a kind of the smoothing filter for the field of graphics. In smoothing method with Gaussian filter input of weighting parameter, value of the target nodes is determined by value of all nodes on the same plane. And the Gaussian filter has the advantage that the extent of the smoothing process is adjustable with the parameter σ. The weighting parameter in Gaussian filter [9] is defined as following equation:

$$G(x, y) = \frac{1}{2\pi\sigma^2} e^{-\frac{x^2+y^2}{2\sigma^2}} \tag{14}$$

where x and y is the distance of x-axial distance and y-axial distance between the target node and referenced node. The weighting parameter becomes large value if the distance is short. The parameter σ which is comparable to the variance in Gaussian distribution determines flattening of the distribution. In addition, as the summation of the weighting parameter for the target node becomes 1, we multiply the weighting parameter by the summation. The weighting parameter for node m to node n is shown in following equation:

$$G^{(m,n)} = \frac{\frac{1}{2\pi\sigma^2} e^{-\frac{(x^{(m)}-x^{(n)})^2+(y^{(m)}-y^{(n)})^2}{2\sigma^2}}}{\sum_{n=1}^{cx} \frac{1}{2\pi\sigma^2} e^{-\frac{(x^{(m)}-x^{(n)})^2+(y^{(m)}-y^{(n)})^2}{2\sigma^2}}} \tag{15}$$

where cx means the number of nodes on the surface, $x^{(m)}$ and $y^{(m)}$ mean x-coordinate and y-coordinate of the node m. Then smoothed gradient vector is computed, the calculating formula is represented as following matrix form:

$$\begin{Bmatrix} \dfrac{\partial J^*}{\partial x^{(1)}}' \\ \dfrac{\partial J^*}{\partial x^{(2)}}' \\ \vdots \\ \dfrac{\partial J^*}{\partial x^{(cx)}}' \end{Bmatrix} = \begin{bmatrix} G^{(1,1)} & G^{(1,2)} & \cdots & G^{(1,cx)} \\ G^{(2,1)} & G^{(2,2)} & \cdots & G^{(2,cx)} \\ \vdots & \vdots & \ddots & \vdots \\ G^{(cx,1)} & G^{(cx,2)} & \cdots & G^{(cx,cx)} \end{bmatrix} \begin{Bmatrix} \dfrac{\partial J^*}{\partial x^{(1)}} \\ \dfrac{\partial J^*}{\partial x^{(2)}} \\ \vdots \\ \dfrac{\partial J^*}{\partial x^{(cx)}} \end{Bmatrix} \tag{16}$$

4.2 Shape identification introducing Gaussian filter

In the Gaussian filter, the parameter σ is given as 20, and the shape identification analysis is carried out. The identified shape of the cavity is shown in Figure 11 (a). The surface of the cavity is smoother than the result without smoothing process in previous section. As the variation of performance function, in the case using Gaussian filter, number of iteration is larger and performance function is lower (See Figure 11(b)). It is confirmed that the temperature comes closer to observed value by applying smoothing process.

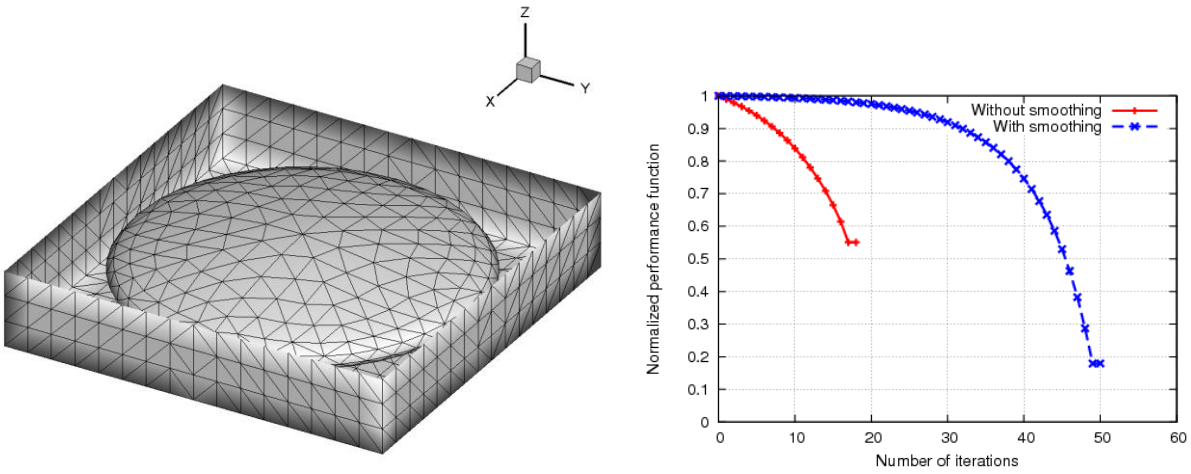

(a) The shape of the cavity at the final iteration

(b) Variation of performance function

Figure 11: Computational results (2)

5 CONCLUSIONS

In this study, the shape identification problem of the cavity in the structure based thermal testing method is carried out. The test piece including a cavity that the shape is variable made by 3D printer is heated from undersurface and the temperature is observed. The shape identification analysis, based the finite element method for four-node tetrahedral element and adjoint variable method, discretizing equations spatially and temporally with Galerkin method and Crank-Nicolson method, is carried out. In the identification process, Gaussian filter is employed to smooth the movement of nodes. The results in this study are shown below.

- When the test piece is heated from lower surface, the temperature of the test piece including a cavity is higher than the one without cavity at the same observation point and time, the temperature at face just above the cavity is especially high.
- The temperature history of the test piece on heating changes depending on the cavity size, the temperature becomes highly as the cavity is larger.

- Using Gaussian filter and smoothing gradient vector, the identified shape of the cavity is smoother than the result without smoothing process, and calculated temperature comes closer to observed temperature.

REFERENCES

[1] T. Kurahashi, H. Oshita, Evaluation of 3D Reinforcement Corrosion Shape in Concrete Based on Observed Temperature on Concrete Surface, *International Journal of Computer Science*, 4:4:340-351, 2010.

[2] T.Kurahashi, H.Oshita, Shape Determination of 3-D Reinforcement corrosion in Concrete Based on Observed Temperature on Concrete Surface, *Computers and Concrete*, 7:1:63-81, 2010.

[3] Z. Wang, I.M. Navon, X. Zou, F.X. Le Dimet, The second order adjoint analysis: theory and applications, *Meteo. and Atmo. Phys*. 50:3-20, 1992.

[4] Z. Wang, I.M. Navon, X. Zou, F.X. Le Dimet, A truncated Newton optimization algorithm in meteorology applications with analytic Hessian/vector products., *Computational Optimization and Applications*, 4:241-262, 1995.

[5] T. Kurahashi, M. Kawahara, Examinations for thermal condition of Lagrange multiplier for heat transfer control problems, *International Journal for Numerical Methods in Engineering*, 73:982-1009, 2008.

[6] T. Kurahashi, Examination for adjoint boundary conditions in initial water elevation estimation problems, *International Journal for Numerical Methods in Fluids*, 63:1270-1295, 2010.

[7] Y. Sakawa, Y. Shindo, On global convergence of an algorithm for optimal control, *IEEE Transactions on Automatic Control*, 25:1149-1153, 1980.

[8] S. Wang, W. Li, Y. Wang, Y. Jiang, S. Jiang, R. Zhao, An improved Difference of Gaussian Filter in Face Recognition, *Journal of Micromechanics and Microengineering*, 7.6.429-433, 2012.

[9] H. Ishiwata, H. Kubota, Y. Shima, Experimental study on Gaussian filter in restoration of error diffused character images, *Information Processing Society of Japan*, 18, 5, 2006.